Design and Experimental Evaluation of a Small-Scale Pumped Storage Hydropower System with a Low-Head Pelton Turbine Integrated with an Off-Grid Solar PV System

Gde KM Atmajaya[1], **Harry Yuliansyah**[2], **Ali Muhtar**[3]
Institut Teknologi Sumatera, Lampung, Indonesia
E-mail : gde.atmajaya@el.itera.ac.id[1], harry.yuliansyah@ el.itera.ac.id [2], ali.muhtar@ el.itera.ac.id [3]
Received 9 April 2026; Revised 22 April 2026; Accepted 24 April 2026

Abstract - This study presents the design and experimental evaluation of a small-scale pumped-storage hydropower (PSH) system integrated with an off-grid photovoltaic (PV) system, serving as a proof-of-concept energy storage prototype. The proposed system consisted of an 800 Wp PV array, an upper and lower reservoir, a low-head Pelton turbine, a DC generator, piping, and a water pump. The system was implemented in a building-based configuration with an effective storage head of 14.65 m. The research was conducted using an engineering design approach, including site assessment, turbine design, turbine-generator testing, PSH-PV integration, and system performance evaluation. The PV subsystem showed a positive linear relationship between solar irradiance and PV output power, indicating an appropriate electrical response under field operating conditions. During the charging test, the nominal 550 L upper reservoir was filled with an actual water volume of 462 L, resulting in a stored potential energy of 18.44 Wh. The estimated electrical input energy required for charging was 105.30 Wh, corresponding to a storage efficiency of 17.51%. During the discharge test, the turbine-generator unit operated for approximately 0.61 h while the tank was being emptied and produced an electrical output energy of 5.76 Wh. DC output power generally ranged from 8.46 W to 10.03 W during the main discharge phase before dropping sharply near the end of operation. The turbine-generator efficiency was 31.24%, while the overall recoverable efficiency of the integrated PSH system was 5.47%. The results confirm the technical feasibility of the proposed PSH-PV system as a small-scale energy storage prototype. However, the relatively low storage efficiency and overall recoverable efficiency indicate that further optimization is required before practical implementation.

Keywords: Pumped Storage Hydropower, Pelton Turbine, Renewable Energy, Photovoltaic System, Energy Storage

1. INTRODUCTION

Electrical energy has become one of the most essential forms of energy in supporting modern human activities. In Indonesia, electricity demand is projected to continue increasing in line with economic and technological development. According to the 2021–2030 Electricity Supply Business Plan (RUPTL), national electricity demand is expected to grow at an average rate of 4.9% per year. In the same plan, renewable energy is targeted to contribute 23% of the national energy mix, while renewable-based power plants account for 51.6% of the planned new generation capacity [1]. In this context, solar photovoltaic (PV) systems have received increasing attention because of their modularity, wide availability, and suitability for distributed and residential-scale energy applications [2], [3], [4], [5].

Based on their configuration, solar PV systems can generally be classified into grid-connected and off-grid systems. In off-grid applications, an energy storage unit is required to maintain power supply continuity when solar irradiation is unavailable, particularly at night or during cloudy conditions. Battery energy storage systems are widely used for this purpose because of their high efficiency, fast response, and relatively simple operation. However, batteries also present several limitations, including relatively high investment cost, performance degradation

e-ISSN : 2356-2579 | p-ISSN : 1412-2693, DOI : 10.62411/tc.v25i2.15971

over time, limited service life, and environmental concerns related to material use and end-of-life disposal [6].

Among the available energy storage technologies, pumped storage hydropower (PSH) is recognized as a mature and reliable option for renewable and hybrid energy systems. It stores surplus electrical energy in the form of gravitational potential by pumping water from a lower reservoir to an upper reservoir during periods of excess electricity generation, and reconverts it into electrical energy when required[7], [8]. However, conventional PSH systems are generally developed at large capacities, require favorable topographical conditions, and often involve long development periods, which limit their direct implementation in small-scale residential photovoltaic (PV) systems [9]. Therefore, recent studies have explored low-head and distributed PSH concepts to extend their applicability to smaller-scale energy storage systems[9], [10], [11].

Previous studies have demonstrated that the integration of photovoltaic (PV) systems with pumped storage hydropower (PSH) provides significant technical and economic potential, especially in locations where sufficient elevation differences exist and the system can be implemented at small to medium scales [12], [13], [14], [15]. However, experimental studies on small-scale, building-based PSH systems employing a low-head Pelton turbine remain limited[16], [17]. Therefore, this study aims to design and experimentally implement a small-scale pumped storage hydropower system integrated with a 800 Wp household-scale off-grid solar PV system. The proposed system consists of upper and lower reservoirs, a low-head Pelton turbine, a DC generator, piping, and a water pump. The system performance is evaluated by storing excess PV energy through water pumping and recovering electrical energy through turbine-driven generation when the PV system is unable to produce electricity.

2. RESEARCH METHOD

2.1 Research Design

This study employed an engineering design approach to develop and evaluate a small-scale pumped storage hydropower (PSH) system integrated with a household-scale photovoltaic (PV) system. The research procedure consisted of five main stages: (1) site assessment and determination of reservoir placement, (2) design of a low-head Pelton turbine, (3) testing of the turbine and generator, and (4) integration of the PSH system with the PV system.

2.2 Site Assessment and Hydraulic Parameter Determination

The first stage involved assessing the installation site to determine the feasibility of implementing the PSH system within the selected building environment. Building D of Institut Teknologi Sumatera was selected because it provides sufficient elevation difference for the placement of the upper and lower reservoirs. The upper reservoir was positioned at the higher elevation level of the building, while the lower reservoir was placed at the ground level. The reservoir arrangement is shown schematically in Figure 1.

e-ISSN : 2356-2579 | p-ISSN : 1412-2693, DOI : 10.62411/tc.v25i2.15971

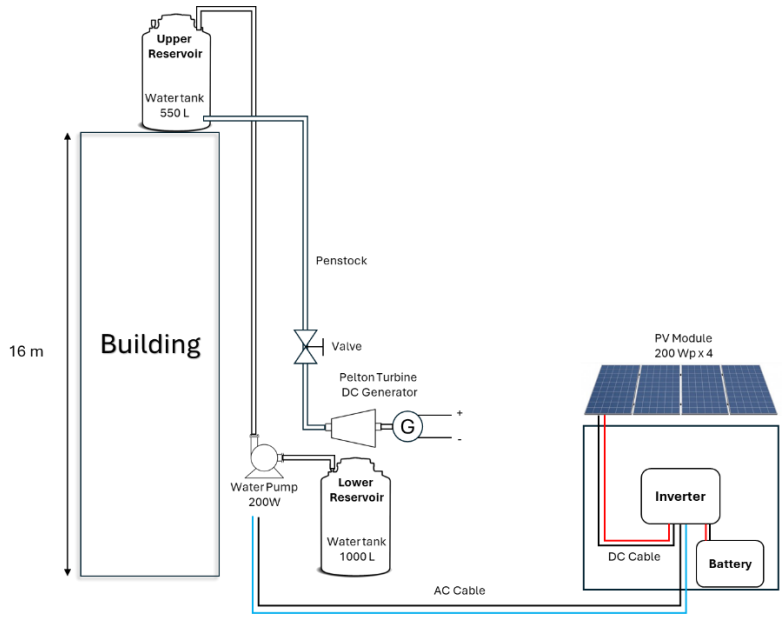

Figure 1. Schematic of the proposed PSH–PV system

The available hydraulic head was determined from the elevation of the selected building location. The building height used in this study was 16 m. Since the upper water tank structure had a height of 1.35 m, the effective head was calculated by subtracting the tank height from the building elevation, as expressed in (1):

$$H_e = H_b - H_t \quad (1)$$

where H_e is the effective head (m), H_b is the building elevation (m), and H_t is the tank height (m). Based on the measured dimensions:

$$H_e = 16 - 1.35 = 14.65 \text{ m}$$

The theoretical hydraulic power available in the system was estimated using:

$$P_h = \rho . g . Q . H_e \quad (2)$$

where P_h is the hydraulic power (W), ρ is the water density (kg/m^3), g is the gravitational acceleration (m/ s^2), Q is the water discharge (m^3/s), and H_e is the effective head (m).
The theoretical electrical output power of the turbine-generator set was estimated by:

$$P_e = \eta_t . \eta_g . \rho . g . Q . H_e \quad (3)$$

where $P_e$is the electrical output power (W), η_t is the turbine efficiency, and η_g is the generator efficiency. The potential energy stored in the upper reservoir was determined by:

$$E_p = \rho . g . V . H_e \quad (4)$$

where E_p is the stored potential energy (J) and V is the useful water volume in the upper reservoir (m^3). For convenience, the stored energy in watt-hours may be obtained from:

$$E_{Wh} = \frac{\rho . g . V . H_e}{3600} \quad (5)$$

e-ISSN : 2356-2579 | p-ISSN : 1412-2693, DOI : 10.62411/tc.v25i2.15971

These hydraulic parameters were used as the basis for selecting the turbine design, estimating the possible electrical output, and determining the feasibility of operating the PSH prototype under the available head condition.

2.3 Low-Head Pelton Turbine Design

The second stage focused on the design of the low-head Pelton turbine as the prime mover for the PSH system. The Pelton turbine was selected in this study because it is relatively simple to design and fabricate, has comparatively low manufacturing cost for a laboratory-scale prototype, and can operate under limited water discharge conditions. Although Pelton turbines are more commonly associated with high-head applications, the use of a low-head Pelton configuration in this study was intended as a proof-of-concept approach for small-scale PSH implementation under the available site conditions of 14.65 m. In addition, the impulse-type working principle was considered advantageous for experimental purposes because it allows direct observation of the relationship between water jet quality, runner rotation, and generator output[18], [19], [20].

The turbine was designed based on the effective head and design discharge obtained from the site assessment stage. The design process included the determination of jet velocity, nozzle dimensions, runner speed, runner diameter, and bucket geometry [21][22][23]. The jet velocity $v_j$at the nozzle outlet was estimated from the effective head H using

$$v_j = C_v\sqrt{2gH} \qquad (6)$$

The discharge through the nozzle was then expressed as

$$Q = A_j v_j \qquad (7)$$

with $A_j$denoting the jet area. The jet area was calculated by

$$A_j = \frac{\pi d_j^2}{4} \qquad (8)$$

in which $d_j$represents the jet diameter [9], [10]. The runner peripheral speed u was estimated using the speed ratio relation

$$u = \phi v_j \qquad (9)$$

where ϕ denotes the speed ratio coefficient. The runner diameter D was determined from the rotational speed N according to

$$u = \frac{\pi DN}{60} \qquad (10)$$

which gives

$$D = \frac{60u}{\pi N} \qquad (11)$$

The jet ratio was used as an additional design reference and defined by

$$m = \frac{D}{d_j} \qquad (12)$$

e-ISSN : 2356-2579 | p-ISSN : 1412-2693, DOI : 10.62411/tc.v25i2.15971

where m denotes the jet ratio between the runner diameter and the jet diameter [10], [11]. The number of buckets was estimated using the empirical expression

$$Z = 15 + \frac{D}{2d_j} \qquad (13)$$

and the calculated value of Z was rounded to the nearest integer for fabrication [10], [11]. The bucket dimensions were selected using empirical ratios with respect to the jet diameter. The bucket width B, bucket length L, and bucket depth T were estimated as

$$B \approx 3.1d_j \text{ to } 3.4d_j \qquad (14)$$
$$L \approx 2.3d_j \text{ to } 2.8d_j \qquad (15)$$
$$T \approx 0.8d_j \text{ to } 1.0d_j \qquad (16)$$

following practical Pelton turbine design recommendations reported in the literature [23][24]. These parameters were selected to ensure stable turbine operation under low-head conditions and to maximize the conversion of hydraulic energy into rotational motion. The final turbine runner design is presented in Figure 2.

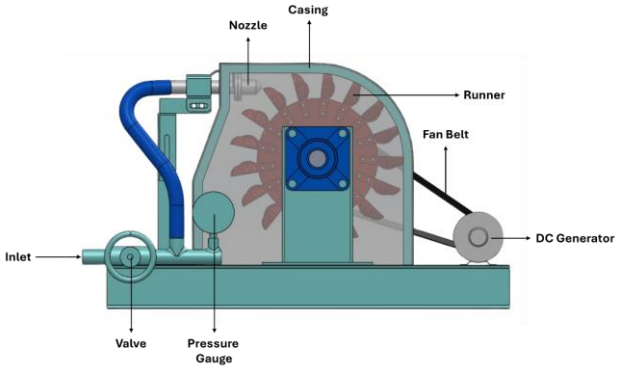

Figure 2. Low-head Pelton turbine set

2.4 Turbine and Generator Testing

After the turbine had been fabricated, experimental testing of the turbine and generator was conducted to evaluate the mechanical and electrical performance of the prototype. In this stage, water was supplied to the turbine at the predetermined discharge, and the turbine rotational speed was measured using a tachometer.

The turbine shaft was mechanically coupled to a DC generator so that the rotational energy produced by the turbine could be converted into electrical energy. The generator output voltage and current were measured using a multimeter. The electrical output power was then calculated as:

$$P_{out} = V_{out} I_{out} \qquad (17)$$

where P_{out} is the electrical output DC power (W), V_{out} is the output voltage (V), and I_{out} is the output current (A). To evaluate the performance of the turbine-generator unit, the conversion efficiency can be estimated by:

$$\eta_{tg} = \frac{P_{out}}{P_h} \times 100\% \qquad (18)$$

e-ISSN : 2356-2579 | p-ISSN : 1412-2693, DOI : 10.62411/tc.v25i2.15971

where η_{tg} is the turbine-generator efficiency (%). This stage was intended to verify whether the developed turbine-generator unit was capable of producing usable electrical output under the available hydraulic conditions.

2.5 Integration of the PSH System with the PV System

In the fourth stage, the PSH prototype was integrated with the household-scale PV system. The PV system used in this study had an installed capacity of 800 Wp and supplied electrical energy to an AC water pump during periods of solar energy availability. The pump was used to transfer water from the lower reservoir to the upper reservoir, thereby converting electrical energy into stored gravitational potential energy.

The pump used in this study operated at 220 V single-phase AC, with a rated power of 200 W and a maximum capacity of 12.6 m^3/h. The charging process of the PSH system was therefore represented by the water pumping process from the lower reservoir to the upper reservoir. The theoretical reservoir filling time can be estimated by[13], [15]:

$$t_f = \frac{V}{Q_p} \quad (19)$$

where t_f is the filling time (h), V is the water volume pumped into the reservoir (m^3), and Q_p is the pump flow capacity (m^3/h).

In practice, the actual filling time was evaluated experimentally because the real pumping performance may be affected by head conditions, piping arrangement, and pump operating characteristics. This stage was intended to examine the compatibility of the PSH prototype with the PV system under charging conditions.

3. RESULTS AND DISCUSSION

3.1 Off-Grid PV System Design

The off-grid photovoltaic (PV) subsystem used in this study consisted of four PV modules connected in series, each rated at 200 Wp, resulting in a total installed capacity of 800 Wp. Each module had a maximum voltage of 36 V and a maximum current of 5.56 A. The DC power generated by the PV array was processed using a 3000 W hybrid inverter with an optimal operating voltage range of 120–550 V. In addition, the system was equipped with a 48 V, 100 Ah LiFePO4 battery to store excess electrical energy and support system operation when solar energy was unavailable. Electrical protection devices were installed on both the DC and AC sides to ensure safe operation.

The PV subsystem was evaluated under field operating conditions by measuring solar irradiance, PV string voltage, and PV string current. The PV output power was then determined from the measured voltage and current values. The relationship between solar irradiance and PV output power is presented in Figure 3.

e-ISSN : 2356-2579 | p-ISSN : 1412-2693, DOI : 10.62411/tc.v25i2.15971

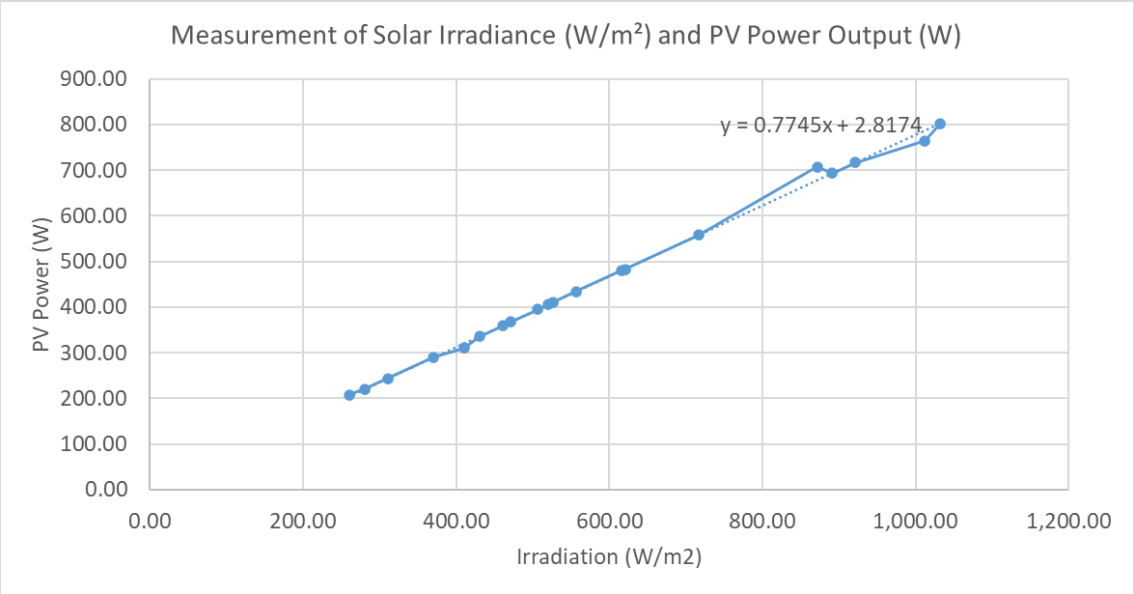

Figure 3. Relationship between solar irradiance and PV output power of the off-grid PV

As shown in Figure 3, the PV output power increased with increasing solar irradiance, indicating a positive linear relationship between the two variables. Within the measured irradiance range of approximately 260 to 1012 W/m², the PV output power increased from about 207 W to 764 W. This result indicates that the PV subsystem responded appropriately to variations in solar radiation under actual operating conditions.

The linear trendline equation, y=0.7745x+2.8174, indicates a positive relationship between solar irradiance and PV output power. In this study, the irradiance data were obtained from the irradiance sensor monitored through the FusionSolar system, while the module surface temperature varied from 24.94 °C at 06:00 to a maximum of 51.32 °C at 11:00, before gradually decreasing to 26.76 °C at 18:00. These conditions should be taken into account when interpreting the irradiance–power relationship, since PV output is influenced not only by solar irradiance but also by module operating temperature.

Although minor deviations from the trendline were observed, these differences may be attributed to several factors, including PV module temperature, atmospheric conditions during measurement, solar incidence angle, and measurement uncertainty. Overall, the results confirm that the off-grid PV subsystem exhibited the expected operating behavior, in which higher solar irradiance resulted in greater electrical power output.

3.2 Reservoir Configuration, Pump Charging Performance, and Energy Storage Analysis

The proposed pumped storage hydropower (PSH) subsystem employed an upper reservoir and a lower reservoir to enable energy storage and recovery through water circulation. The nominal capacity of the upper reservoir was 550 L. However, during the pump charging test, the reservoir was not filled to its full capacity, and the actual volume of water transferred to the upper reservoir was 462 L, equivalent to 0.462 m³. Therefore, the energy storage analysis in this subsection was based on the actual stored water volume rather than the nominal tank capacity.

For the PSH system analysis, the effective storage head was taken as 14.65 m, corresponding to the vertical elevation difference used in the system design. Based on the actual stored water volume and the effective storage head, the theoretical stored potential energy was calculated using equation (4). Using the measured parameters, the stored potential energy in the upper reservoir was 18.44 Wh. This value represents the theoretical maximum useful energy stored in the form of gravitational potential energy under the actual charging condition.

A pump charging test was then conducted to evaluate the charging performance of the system. During the test, the filling process required 1670 s, or 0.464 h, with a pump rotational

e-ISSN : 2356-2579 | p-ISSN : 1412-2693, DOI : 10.62411/tc.v25i2.15971

speed of 1415 rpm. Based on the transferred water volume and filling duration, the average discharge during charging was approximately 0.277 L/s. The main results of the pump charging test are summarized in Table 1.

Table 1. Summary of pump charging test and energy storage performance.

Parameter	Value
Actual stored water volume, $V(L)$	462
Filling time, $t_f(h)$	0.464
Average discharge, $Q(L/s)$	0.277
Effective PSH storage head, $H(m)$	14.65
Stored potential energy, $E_p(W_h)$	18.44
Estimated electrical input energy, $E_p(W_h)$	105.3
Storage efficiency, $\eta(\%)$	17.51

As shown in Table 1, the estimated electrical input energy required during the charging process was 105.3 Wh, calculated from the measured pump voltage, current, and charging duration. Compared with the stored potential energy of 18.44 Wh, the resulting storage efficiency was 17.51%. This result indicates that only a relatively small portion of the supplied electrical energy was converted into useful stored gravitational potential energy in the upper reservoir.
The relatively low storage efficiency suggests that substantial losses occurred during the charging process. These losses may be associated with pump inefficiency, friction losses in the piping system, minor losses in fittings and valves, and uncertainty in estimating the actual electrical input energy based solely on voltage and current measurements. Nevertheless, the charging test confirms that the proposed PSH subsystem was capable of storing electrical energy in the form of gravitational potential energy. For more accurate evaluation, future tests should include direct measurement of the pump's real power consumption using a wattmeter or power analyzer.

3.3 Turbine–Generator Performance

The low-head Pelton turbine designed in this study was tested together with the generator to evaluate its ability to convert hydraulic energy into electrical energy during the discharge process. During the test, water from the upper reservoir was released to drive the turbine, and the turbine rotational speed, pressure, output voltage, output current, and DC output power were measured at several time intervals.

The measured data indicate that the turbine–generator unit operated relatively stably during most of the discharge period. The turbine rotational speed was generally maintained within the range of approximately 190–207 rpm, while the generator output voltage varied from 26.6 to 29.4 V and the output current remained between 0.31 and 0.34 A. Under these conditions, the DC output power was generally maintained in the range of 8.46–10.03 W, indicating stable electrical output during the main discharge phase.

The variation of DC output power with discharge time is shown in Figure 4. As can be observed, the output power remained relatively stable during most of the test period, with only minor fluctuations. However, a sharp decline occurred near the end of the discharge process, where the output power dropped to 1.69 W and 1.56 W. This behavior indicates that the available hydraulic energy became insufficient to sustain stable turbine–generator operation as the upper reservoir approached depletion.

e-ISSN : 2356-2579 | p-ISSN : 1412-2693, DOI : 10.62411/tc.v25i2.15971

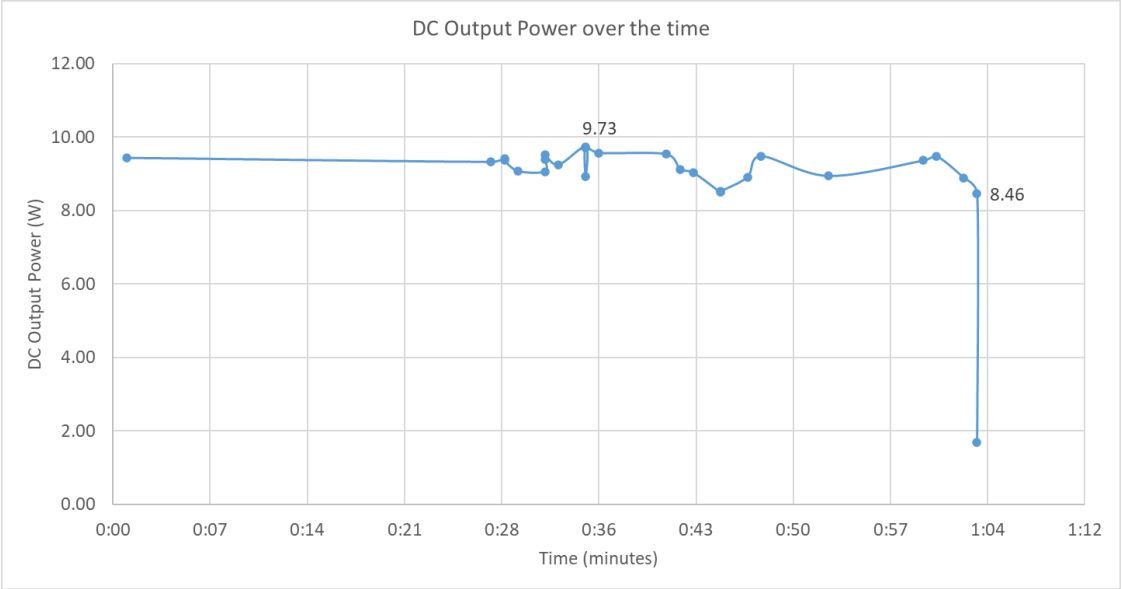

Figure 4. DC output power as a function of discharge time during turbine–generator testing.

A similar trend can be observed in Figure 5, which presents the turbine rotational speed as a function of discharge time. During most of the discharge period, the turbine rotational speed remained relatively stable, indicating that the water flow was still sufficient to maintain turbine operation. Near the end of the test, however, the rotational speed dropped significantly to 120 rpm and then to 90 rpm. This reduction in rotational speed explains the corresponding decrease in output voltage and power observed at the final stage of discharge.

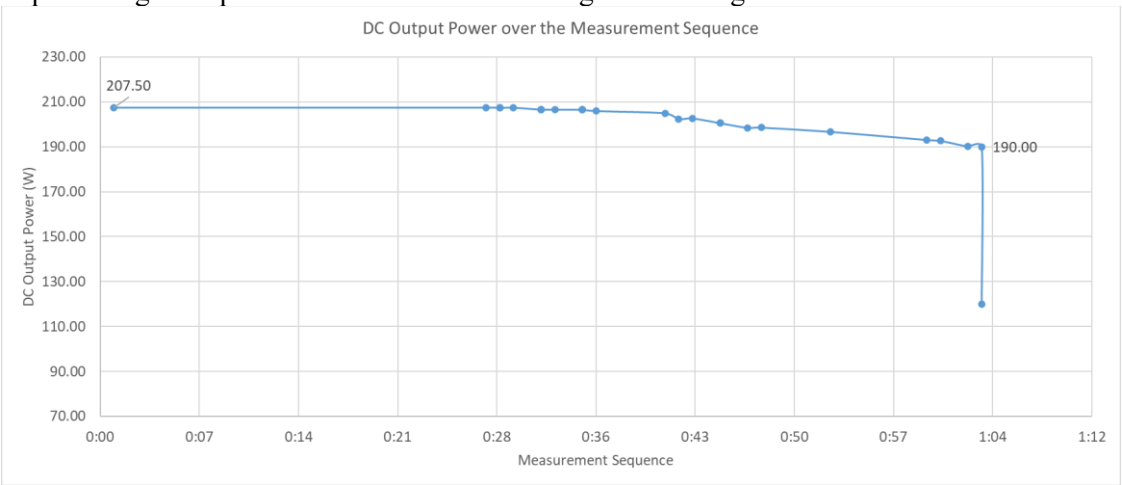

Figure 5. Turbine rotational speed as a function of discharge time.

The relationship between turbine rotational speed and DC output power is illustrated in Figure 6. The graph shows that higher rotational speed generally resulted in higher electrical output power. This confirms that the generator performance was strongly influenced by the mechanical input provided by the turbine. Therefore, maintaining a stable turbine speed is essential for achieving stable electrical output in the proposed PSH system.

e-ISSN : 2356-2579 | p-ISSN : 1412-2693, DOI : 10.62411/tc.v25i2.15971

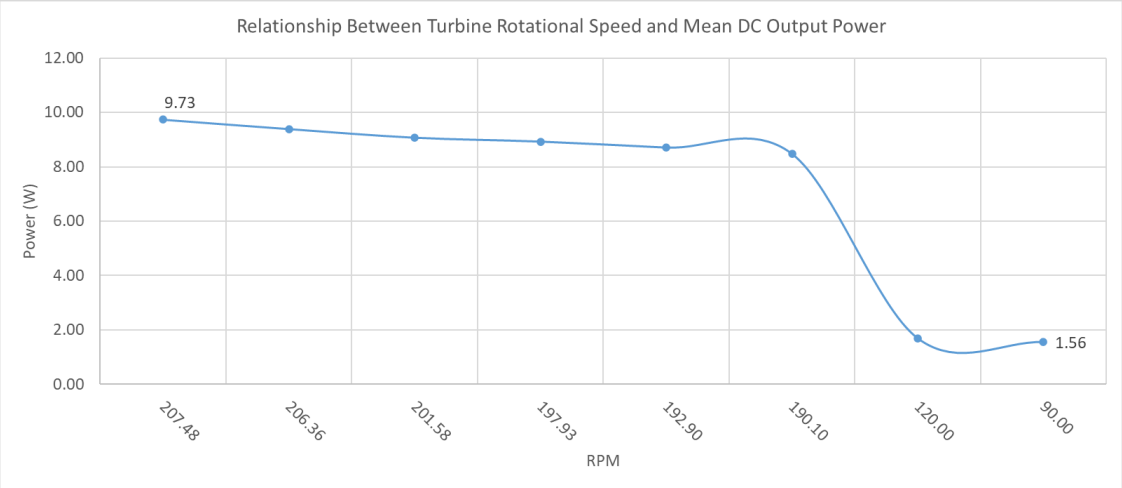

Figure 6. Relationship between turbine rotational speed and DC output power.

Overall, the test results demonstrate that the turbine–generator unit was capable of producing usable DC electrical power during the discharge process. The results also show that the prototype had a relatively stable operating region during most of the test, followed by a rapid performance drop near the end of discharge. During the initial discharge stage, corresponding approximately to an upper reservoir volume range of 60–100%, the turbine operated under relatively stable conditions, with a maximum rotational speed of 207.50 rpm and a maximum DC output power of 9.73 W. This indicates that when a sufficient water volume was still available in the upper reservoir, the system was able to maintain stable turbine rotation and electrical output. As the water volume decreased, both the rotational speed and DC output power gradually declined, followed by a sharp drop near the end of discharge. This behavior is characteristic of a small-scale storage system in which the available hydraulic energy decreases as the stored water is depleted. Although the system performance was still limited, the test confirms the technical feasibility of using the developed low-head Pelton turbine as part of a small-scale PSH prototype. For further improvement, future work should focus on optimizing the turbine–generator matching, reducing hydraulic and mechanical losses, and conducting repeated tests under different discharge conditions to obtain a more comprehensive performance curve.

3.4 Integration of the PSH System with the PV System

The integration of the pumped storage hydropower (PSH) system with the photovoltaic (PV) system was evaluated to determine the overall energy recovery from the charging and discharge processes. In this configuration, electrical energy from the PV subsystem was used to pump water to the upper reservoir, where it was stored as gravitational potential energy and later recovered as electrical energy through the turbine–generator unit.

Based on the charging test in Subsection 3.2, the electrical input energy supplied to the pump was 105.30 Wh, while the stored potential energy in the upper reservoir was 18.44 Wh. Therefore, the storage efficiency was 17.51%. During the discharge test in Subsection 3.3, the turbine–generator unit produced an electrical output energy of 5.76 Wh as illustrated in Figure 7. Accordingly, the turbine–generator efficiency was 31.24%, and the overall recoverable efficiency of the integrated PSH system was calculated as

$$\eta_{total} = \frac{E_{out}}{E_{in}} \times 100\% \qquad (17)$$

Thus,

$$\eta_{total} = \frac{5.76}{105.30} \times 100\% = 5.47\% \qquad (18)$$

e-ISSN : 2356-2579 | p-ISSN : 1412-2693, DOI : 10.62411/tc.v25i2.15971

These results indicate that the proposed PSH–PV configuration was technically capable of storing and recovering electrical energy, although the overall efficiency remained low. The limited efficiency is likely caused by cumulative losses in the pump, piping system, turbine, and generator.

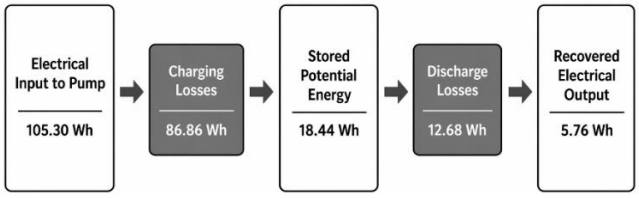

Figure 7. Energy flow of the integrated PSH–PV system from pump input to recovered electrical output

One important factor contributing to the low efficiency is the penstock configuration. In the present prototype, the penstock layout was not fully optimized because the flow path included three 90° elbows and a sudden contraction before the nozzle inlet. This configuration likely increased local losses, disturbed flow uniformity, and reduced the effective jet momentum delivered to the turbine runner. To minimize such losses, the penstock should ideally provide the shortest and smoothest possible flow path, with minimal bends, fittings, and abrupt diameter changes. Overall, the integrated test confirms the feasibility of combining the PV subsystem with the PSH prototype as a small-scale short-duration energy storage system. However, further improvement is required, particularly in pump performance, penstock design, turbine–generator matching, and load-side electrical conditioning, in order to increase the overall system efficiency.

4. CONCLUSION

This study presented the design and experimental evaluation of a small-scale pumped storage hydropower (PSH) system integrated with an off-grid photovoltaic (PV) system. The proposed system consisted of an 800 Wp PV subsystem, an upper and lower reservoir, a low-head Pelton turbine, a generator, and a pump for the charging process. The study was intended to examine the feasibility of using a building-based PSH configuration as a small-scale energy storage prototype.

The results showed that the off-grid PV subsystem responded appropriately to variations in solar irradiance, where higher irradiance produced higher PV output power. The pump charging test demonstrated that electrical energy could be stored in the form of gravitational potential energy by transferring water to the upper reservoir. Although the nominal upper reservoir capacity was 550 L, the actual water volume stored during the charging test was 462 L. Based on the effective storage head of 14.65 m, the stored potential energy was 18.44 Wh, while the estimated electrical input energy during charging was 105.30 Wh, resulting in a storage efficiency of 17.51%.

The turbine-generator test further showed that the developed low-head Pelton turbine was capable of converting the stored hydraulic energy into electrical energy. During the discharge process, the turbine-generator unit operated relatively stably over most of the test period, with DC output power generally ranging from 8.46 W to 10.03 W before dropping sharply near the end of discharge. The electrical output energy recovered during discharge was 5.76 Wh, corresponding to a turbine-generator efficiency of 31.24%. Overall, the integrated PSH-PV system achieved an overall recoverable efficiency of 5.47%, indicating that only a small portion of the initial electrical input energy used during charging could be recovered again as electrical output during discharge. These results confirm the technical feasibility of the proposed PSH-PV system as a small-scale energy storage prototype. However, the relatively low storage efficiency and overall recoverable efficiency indicate that the current system remains at the proof-of-concept stage and requires further improvement before practical implementation. Future work should focus on improving

e-ISSN : 2356-2579 | p-ISSN : 1412-2693, DOI : 10.62411/tc.v25i2.15971

pump efficiency, optimizing turbine-generator matching, reducing hydraulic losses, and performing more comprehensive integrated load testing under different operating conditions.

REFERENCES

[1] R. Patriamurti, H. Sasana, and J. A. Prakoso, "ANALISIS PERTUMBUHAN EKONOMI, PERTUMBUHAN INDUSTRI, PERTUMBUHAN PENDUDUK, PENGELUARAN KONSUMSI, DAN INVESTASI ASING TERHADAP KONSUMSI LISTRIK DI INDONESIA TAHUN 1971-2019," *DINAMIC : Directory Journal of Economic*, vol. 4, pp. 852–871, 2021, doi: https://doi.org/10.31002/dinamic.v3i4.2723.

[2] H. Sun *et al.*, "Study on the performance and economy of the building-integrated micro-grid considering photovoltaic and pumped storage: A case study in Foshan," *International Journal of Low-Carbon Technologies*, vol. 17, pp. 630–636, 2022, doi: 10.1093/ijlct/ctac039.

[3] Y. Lahmer, A. Chaker, and A. Nedjar, "Performance evaluation of grid-connected photovoltaic with pumped hydro storage system in high-rise building," *Energy for Sustainable Development*, vol. 81, p. 101470, 2024, doi: 10.1016/j.esd.2024.101470.

[4] N. Mousavi, G. Kothapalli, D. Habibi, C. K. Das, and A. Baniasadi, "A novel photovoltaic-pumped hydro storage microgrid applicable to rural areas," *Appl. Energy*, vol. 262, p. 114284, 2020, doi: 10.1016/j.apenergy.2019.114284.

[5] M. Zeidan, Z. Alakayleh, and S. Quasem, "Integrating a Solar PV System with Pumped Hydroelectric Energy Storage for Self-Consumption," *Energies (Basel).*, vol. 16, no. 15, p. 5769, 2023, doi: 10.3390/en16155769.

[6] A. R. Dehghani-Sanij, E. Tharumalingam, M. B. Dusseault, and R. Fraser, "Study of energy storage systems and environmental challenges of batteries," *Renewable and Sustainable Energy Reviews*, vol. 104, pp. 192–208, 2019, doi: 10.1016/j.rser.2019.01.023.

[7] S. Rehman, L. M. Al-Hadhrami, and M. M. Alam, "Pumped hydro energy storage system: A technological review," *Renewable and Sustainable Energy Reviews*, vol. 44, pp. 586–598, 2015, doi: 10.1016/j.rser.2014.12.040.

[8] P. Das, B. K. Das, N. N. Mustafi, and T. Sakir, "A review on pump-hydro storage for renewable and hybrid energy systems applications," *Energy Storage*, vol. 3, no. 4, p. e223, 2021, doi: 10.1002/est2.223.

[9] J. P. Hoffstaedt *et al.*, "Low-head pumped hydro storage: A review of applicable technologies for design, grid integration, control and modelling," *Renewable and Sustainable Energy Reviews*, vol. 158, p. 112119, 2022, doi: 10.1016/j.rser.2022.112119.

[10] A. Boroomandnia, B. Rismanchi, and W. Wu, "A review of micro hydro systems in urban areas: Opportunities and challenges," *Renewable and Sustainable Energy Reviews*, vol. 169, p. 112866, 2022, doi: 10.1016/j.rser.2022.112866.

[11] A. Boroomandnia, B. Rismanchi, W. Wu, and R. Anderson, "Optimal design of micro pumped-storage plants in the heart of a city," *Sustain. Cities Soc.*, vol. 101, p. 105054, 2024, doi: 10.1016/j.scs.2023.105054.

[12] J. Jurasz, A. Piasecki, J. Hunt, W. Zheng, T. Ma, and A. Kies, "Building integrated pumped-storage potential on a city scale: An analysis based on geographic information systems," *Energy*, vol. 242, p. 122966, 2022, doi: 10.1016/j.energy.2021.122966.

[13] S. Balachandran and K. Ponnusamy, "Feasibility of integrated solar photovoltaic pico-pumped storage self-sustained system for multi-storey building in India," *Energy Storage*, vol. 6, p. e601, 2024, doi: 10.1002/est2.601.

[14] X. Xu, W. Hu, D. Cao, Q. Huang, C. Chen, and Z. Chen, "Optimized sizing of a standalone PV-wind-hydropower station with pumped-storage installation hybrid energy system," *Renew. Energy*, vol. 147, pp. 1418–1431, 2020, doi: 10.1016/j.renene.2019.09.099.

e-ISSN : 2356-2579 | p-ISSN : 1412-2693, DOI : 10.62411/tc.v25i2.15971

[15] B. Hammad, S. Al-Dahidi, Y. Aldahouk, D. Majrouh, and S. Al-Remawi, "Technical, Economic, and Environmental Investigation of Pumped Hydroelectric Energy Storage Integrated with Photovoltaic Systems in Jordan," *Sustainability*, vol. 16, no. 4, p. 1357, 2024, doi: 10.3390/su16041357.

[16] N. Guignard, C. Cristofari, V. Debusschere, L. Garbuio, and T. Le Mao, "Micro Pumped Hydro Energy Storage: Sketching a Sustainable Hybrid Solution for Colombian Off-Grid Communities," *Sustainability*, vol. 14, no. 24, p. 16734, 2022, doi: 10.3390/su142416734.

[17] M. Simão and H. M. Ramos, "Hybrid Pumped Hydro Storage Energy Solutions towards Wind and PV Integration: Improvement on Flexibility, Reliability and Energy Costs," *Water (Basel).*, vol. 12, no. 9, p. 2457, 2020, doi: 10.3390/w12092457.

[18] E. Quaranta and C. Trivedi, "The state-of-art of design and research for Pelton turbine casing, weight estimation, counterpressure operation and scientific challenges," *Heliyon*, vol. 7, no. 12, p. e08527, 2021, doi: 10.1016/j.heliyon.2021.e08527.

[19] M. Elgammi and A. A. Hamad, "A feasibility study of operating a low static pressure head micro Pelton turbine based on water hammer phenomenon," *Renew. Energy*, vol. 195, pp. 1–16, 2022, doi: 10.1016/j.renene.2022.05.131.

[20] R. Khan, "Experimental and numerical investigation of hydro Pelton turbine study," *Renew. Energy*, 2024.

[21] Z. Zhang, "Hydraulic Design of Pelton Turbines," in *Pelton Turbines*, Cham, Switzerland: Springer, 2016. doi: 10.1007/978-3-319-31909-4_18.

[22] T. Z. Oo, N. Nyi, and C. C. Khaing, "Design Calculation of Pelton Turbine for 220 kW," *International Journal of Scientific and Research Publications*, vol. 9, no. 7, pp. 218–224, 2019, doi: 10.29322/IJSRP.9.07.2019.p9131.

[23] A. K. Minn, H. H. Win, and N. A. San, "Design of 225kW Pelton Turbine," *International Journal of Scientific Engineering and Technology Research*, vol. 3, no. 24, pp. 4836–4842, 2014.

[24] E. Quaranta and C. Trivedi, "The state-of-art of design and research for Pelton turbine casing, weight estimation, counterpressure operation and scientific challenges," *Heliyon*, vol. 7, no. 12, p. e08527, 2021, doi: 10.1016/j.heliyon.2021.e08527.

e-ISSN : 2356-2579 | p-ISSN : 1412-2693, DOI : 10.62411/tc.v25i2.15971